JOURNAL OF MATERIALS SCIENCE: MATERIALS IN MEDICINE 7 (1996) 439–445

Fabrication of transparent hydroxyapatite and application to bone marrow derived cell/hydroxyapatite interaction observation *in-vivo*

K. TAKIKAWA, M. AKAO
Division of Inorganic Materials, Institute for Medical and Dental Engineering, Tokyo Medical and Dental University, 2-3-10, Surugadai, Kanda, Chiyoda-ku, Tokyo 101, Japan

Transparent hydroxyapatite (HA), 99.6% relative density, was prepared by hot isostatic pressing. Optical transmittance of 1 mm thick HA was greater than 60% at 700 nm. Twenty transparent HA plates (10 × 7 × 1 mm) were implanted into the medullary cavities of two dogs' femora. At 1 and 2 weeks after implantation the bone marrow derived cells that adhered to the HA surfaces were histochemically examined by light microscopy and scanning electron microscopy. Four types of enzymatic reactions were employed to identify cell types. Alkaline phosphatase was used as a marker for osteoblasts, acid phosphatase and tartrate-resistant acid phosphatase as a marker for osteoclasts and non-specific esterase as a marker for macrophages. Cells adhered to the HA surfaces were a mixed population of osteoblasts, osteoclasts and macrophages. By 2 weeks, the number of osteoblasts increased and formed a bone-like matrix. A small number of osteoclasts formed resorption lacunae on the HA after 2 weeks. By utilizing the transparency of the HA, whole-view of bone matrix formation by osteoblasts and simultaneous resorption of HA by osteoclasts was observed simply and dynamically by light microscopy.

1. Introduction

In order to produce transparent polycrystalline ceramics, it is not only necessary to remove all the pores from the ceramic but to inhibit grain growth. Since the hot press (HP) technique was applied to the sintering of ceramics, fabrication of dense ceramics has become easy. Therefore, many investigators have succeeded in sintering transparent polycrystalline ceramics. Aoki obtained transparent HA by applying the HP technique to the sintering of HA [1].

In addition, hot isostatic pressing (HIP) also enables effective densification of ceramics. Fujiwara *et al.* [2] and Ioku *et al.* [3] reported that the post-sintering of HA of HIP'ing brought about densification up to 99% for samples more than 90% dense, and transparent HA were obtained. Aoki *et al.* [4] used transparent HA produced by HIP'ing for cellular observation *in vitro*. They suggested that transparent HA could be a useful material in the observation of HA/cellular, or HA/tissue reactions. Müller-Mai *et al.* [5] investigated the interface of dense HA produced by HIP'ing after implantation into the femur of rabbits by scanning electron microscopy (SEM) and transmission electron microscopy (TEM). They reported that the HIP'ed HA bonded directly with the new bone of the femur, and degradation of the implant material by osteoclast-like cells partially occurred after implantation.

However, no investigations have taken advantage of the transparency of HIP'ed HA *in vivo*. In the present report, by utilizing the transparency of HIP'ed HA, the histochemical interaction between HA and cells in the medullary cavity was observed simply and dynamically by light microscopy, thus avoiding the necessity of histological thin sections.

2. Materials and methods

2.1. Preparation of transparent HA

A suspension of 0.5 M $Ca(OH)_2$ in 1000 ml distilled water was vigorously stirred at room temperature and a solution of 0.3 M H_3PO_4 in 1000 ml distilled water was added in drops to produce a gelatinous precipitate. The resulting slurry was filtered and dried at 80 °C. The products were calcined at 800 °C for 1 h. The finely ground powders, mixed with 3.5 wt % polyvinyl alcohol and 1 wt % triethylene glycohol, were pressed in a mould at a pressure of 78 MPa. The compacts were heated in air at 1100 °C for 2 h. The sintered bodies were HIP'ed (Dr. HIP, Kobelco, Japan) at 1100 °C under 200 MPa of Ar for 1 h.

X-ray diffractometry was carried out on finely ground samples of sintered HA and HIP'ed HA using CuK_α radiation. The relative density was calculated from specimen mass and dimensions measured by a precision balance and vernier caliper; theoretical density of HA was assumed to be 3.16 $Mg\,m^{-3}$. The average grain size was estimated by the linear intercept method using SEM micrographs of the samples after etching in 0.1 M acetic acid solution for 1 min.

0957–4530

Specimens (17 × 4 × 2 mm) were cut from discs of the sintered and HIP'ed bodies with a low-speed diamond saw. Three-point bending tests were performed with a span of 15 mm at a crosshead speed of 0.1 mm min^{-1}. Seven samples were tested for each condition. The morphology of the fracture surfaces was examined by SEM.

2.2. Subcutaneous implantation tests

In vivo change of transmittance in the HIP'ed transparent HA was examined by subcutaneous implantation tests. Specimens (10 × 7 × 1 mm) were cut from discs of the HIP'ed HA with a low-speed diamond saw. Specimens were hand polished with a 2.5 μm diamond paste and transparent HA was obtained. The transmittance was measured by UV-visible spectrophotometer (UV-260, Simazu, Japan). The specimens were ultrasonically washed three times for 30 min in 70% ethanol and sterilized by irradiation with ultraviolet light for 12 h. One adult beagle dog was used in this experiment. Under general anesthesia, skin incisions (10 mm) on the back of the dog were made. Subcutaneous pouches were created by blunt dissection. Ten specimens were implanted in the subcutaneous tissue. At 2 and 4 weeks after implantation, the samples were investigated by transmittance measurement and X-ray diffractometry. After these investigations, the samples were examined by SEM.

2.3. Observation after implantation into medullary cavities

2.3.1. Implantation method

Two adult beagle dogs were used in this experiment. Under general anesthesia, skin incisions were made, muscles and periosteum were retracted, and the femoral diaphysis were exposed. Cavities (7 × 1 mm) penetrating to the medullary space were drilled vertically to the femoral axis using a dental engine. Five cavities were made per femur, and then sterile transparent HA was implanted into the cavities.

At 1 week after implantation, the samples on right side, and after 2 weeks those on left side, were extracted. The samples were washed three times with Hank's balanced salt solution (BSS) containing penicillin 100 IU ml^{-1} and streptomycin sulfate 100 μg ml^{-1}. *In vitro* cultures were carried out in order to confirm that the samples were not contaminated and non-adherent cells were removed. The samples were placed in culture dishes with α-modification of Eagle's minimum essential medium (α-MEM; Gibco, USA) supplemented with 10% fetal bovine serum (Gibco). The culture was maintained at 37 °C in a 5% CO_2 incubator. The samples were observed with a phase-contrast microscope and were harvested for light microscopy after 24 h incubation.

2.3.2. Light microscopy

The samples were rinsed once with BSS and fixed with ethanol: acetone (1 : 1) for alkaline phosphatase (ALP) stain and with methanol: acetone (1 : 1) for acid phosphatase (ACP) stain, tartrate resistant acid phosphatase (TRAP) stain and nonspecific esterase (NSE) stain for 30 min at 4 °C. The following four enzyme reactions were employed for light microscopy:

(1) Staining for ALP was performed according to the azo dyes method of Burstone [6]. The samples were incubated for 30 min at 37 °C in 0.2 M Tris-HCl buffer (pH 8.5) containing naphthol AS-MS phosphate (Sigma, USA) as a substrate and Fast Blue RR salt (Sigma) as a stain for the reaction product.

(2) Staining for ACP was performed according to the fast garnet GBC method [6], incubating the samples for 30 min at 37 °C in 0.1 M sodium acetate buffer (pH 5.2) containing naphthol AS-BI phosphate (Sigma) adding N-N' dimethyl-formamid as a substrate and Fast Garnet GBC salt (Sigma) as a stain for the reaction product. Tartrate resistance was tested by adding 0.05 M sodium tartrate in the incubating medium.

(3) Staining for NSE was performed using a commercially available kit (Sigma) for α-naphthyl acetate esterase. The samples were incubated for 30 min at 37 °C in 0.2 M Tris-HCl buffer (pH 7.6) containing α-naphthyl acetate as a substrate and Fast Blue BB Base as a stain for the reaction product.

After incubation, the samples were counter-stained with 1% methylene blue and observed under a light microscope (Microphot-FXA, Nikon, Japan).

2.3.3. Electron microscopy

The samples were fixed with 2.5% glutaralaldehyde in 0.1 M phosphate buffer (pH 7.3) and post-fixed with 2% osmium tetroxide in 0.1 M phosphate buffer (pH 7.3). They were dehydrated in a graded series of ethanol, treated with isoamyl acetate, critical point dried using liquid CO_2, sputter-coated with platinum, and studied by SEM. After light microscopy observation of TRAP stained samples, they were dipped in 0.25 M NH_4OH for 1 h to remove adherent cells and the surfaces examined using SEM.

3. Results

3.1. Characterization of HIP'ed HA

From the X-ray diffraction patterns, phase change of HA after HIP'ing could not be detected. Additional phases such as tricalcium phosphate could not be detected after subcutaneous implantation, suggesting the pysico-chemical stability of HIP'ed HA.

The relative density and average grain size results are summarized in Fig. 1 and Table I. SEM micrographs (Fig. 2) of etched surfaces of the samples indicated the removal of pores by HIP'ing. However, the average grain size after HIP'ing was the same as before HIP'ing. Normal sintering of HA can not yield microstructures with grain sizes smaller than 0.5 μm with 99% relative density [7, 8]. Thus, HIP'ing appears useful in the fabrication of dense HA with a fine grain size.

The results of mechanical properties are summarized in Table I. Significant difference in Young's

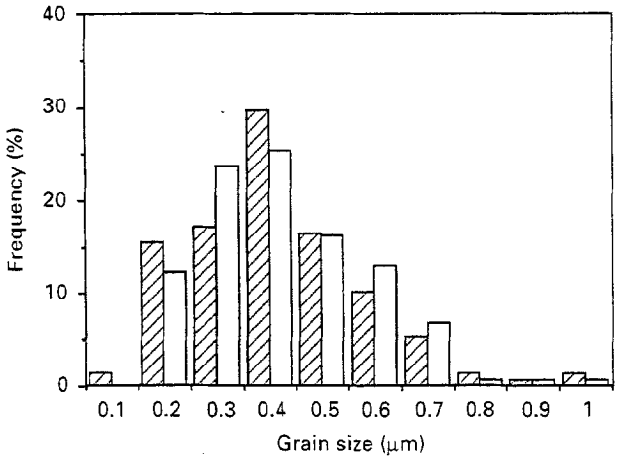

Figure 1 Grain size distributions of 150 grains of sintered (□) and HIP'ed (▨) HA.

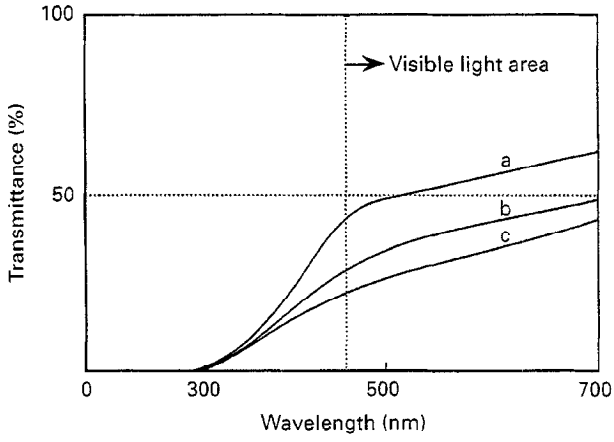

Figure 3 Change in transmittance of 1 mm thick transparent HA (a) before implantation and at (b) 2 and (c) 4 weeks after subcutaneous implantation.

TABLE I Relative density, average grain size, bending strength, and Young's modulus results for sintered and HIP'ed HA

	Relative density (%)	Grain size (μm)	Bending strength (MPa)	Young' modulus (GPa)
Sintered HA	97.6	0.43 ± 0.16	107.5 ± 4.2	84.7 ± 16.5
HIP'ed HA	99.6	0.42 ± 0.17	70.1 ± 1.8	80.6 ± 13.8

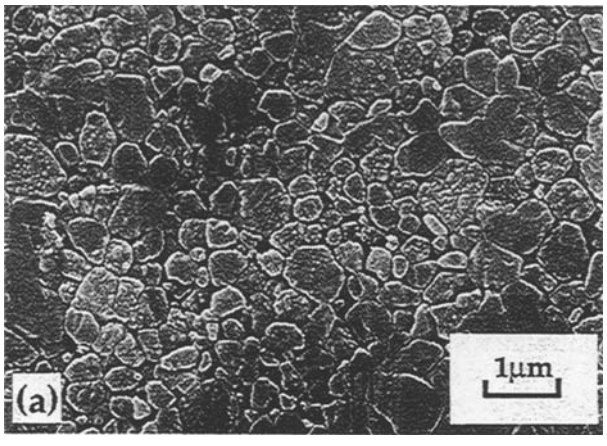

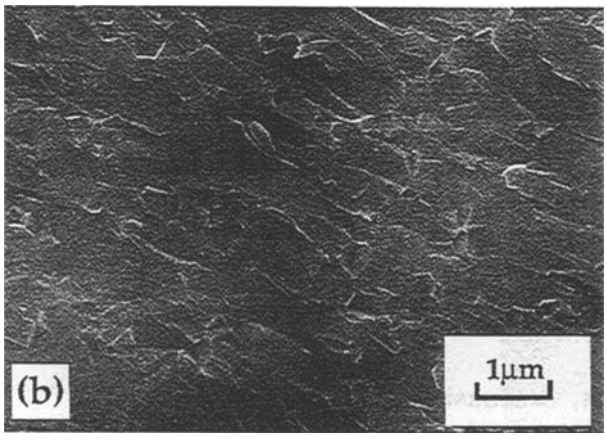

Figure 2 SEM micrographs of etched and fracture surfaces: (a) etched surface of HIP'ed HA; (b) fracture surface of HIP'ed HA.

modulus between before and after HIP'ing were not observed. However, the bending strength decreased after HIP'ing. It is generally agreed that the mechanical properties of brittle polycrystalline ceramics depends on porosity and grain size. No significant difference in Young's modulus may have resulted from the inhibition of the grain growth during HIP'ing. The decrease in bending strength is probably due to the increase of relative density. Fig. 2 shows the fracture surfaces of HIP'ed HA. SEM observation revealed that fracture of HIP'ed HA occurred as a transgranular fracture process. This agreed with the findings of Akao *et al.* [7, 8] that fracture surfaces of dense HA indicate predomination of transgranular failures.

Fig. 3 shows the transmittance of 1 mm thick transparent HA and after 2 and 4 weeks subcutaneous implantation. Fig. 4 shows SEM micrographs of the surface after 2 and 4 weeks subcutaneous implantation. At 2 weeks, dissolution of small grains was observed. This dissolution exposed grain boundaries. At 4 weeks, the dissolution was extensive over the entire sample. In order to obtain transparent ceramics with high transmittance, it is necessary to prevent light dispersion at the surface. The smoother the surface of a transparent polycrystalline ceramic, the higher the transmittance. By polishing with diamond paste, a transmittance of $> 60\%$ was obtained. After subcutaneous implantation, chemical dissolution decreased the transmittance. Thus, the transparent HA showed about 40% transmittance at 4 weeks after subcutaneous implantation. This indicates that transparent HA is suitable for *in vivo* observation.

3.2. Observation of bone marrow derived cells

From phase-contrast microscopy observations (Fig. 5), three types of cells were detected on the samples: spindle-shaped cells, round cells, and multinucleated giant cells (MNGCs).

At 1 week after implantation, the spindle cells contacted with adjacent spindle cells by processes and generally formed a cellular network on the samples. At 2 weeks after implantation, the number of

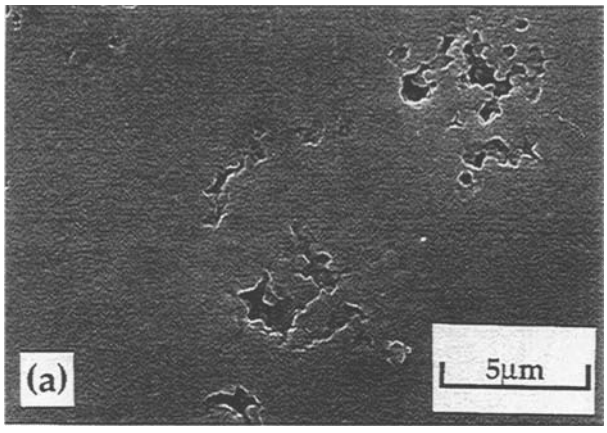

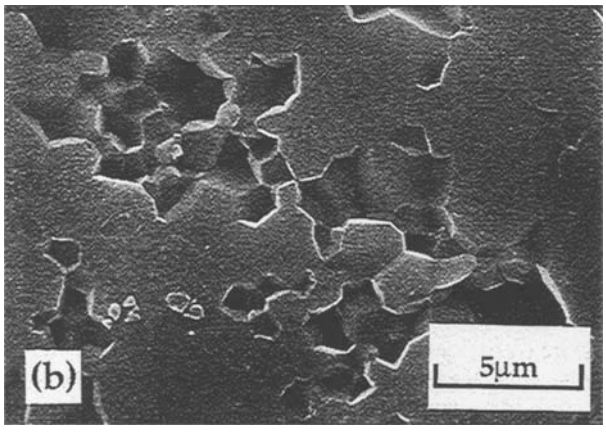

Figure 4 SEM micrographs showing the surface of transparent HA after subcutaneous implantation (a) at 2 weeks; (b) at 4 weeks.

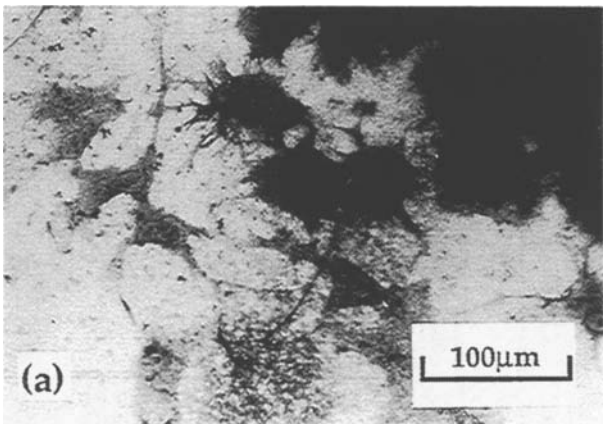

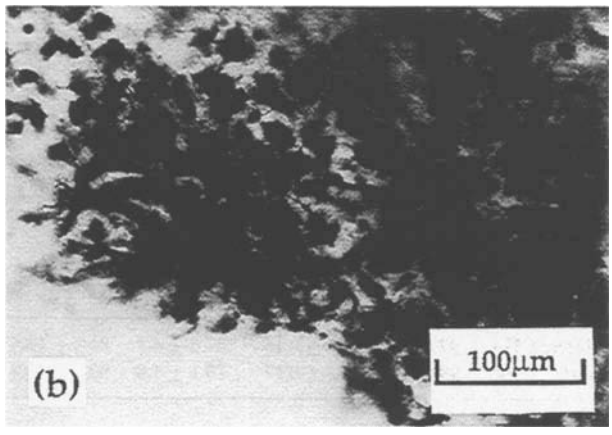

Figure 6 Light microscopy of alkaline phosphatase (ALP) staining: (a) at 1 week, spindle shaped cells displayed ALP activity were in contact with adjacent cells and formed a cellular network; (b) at 2 weeks, these cells formed multiple layers.

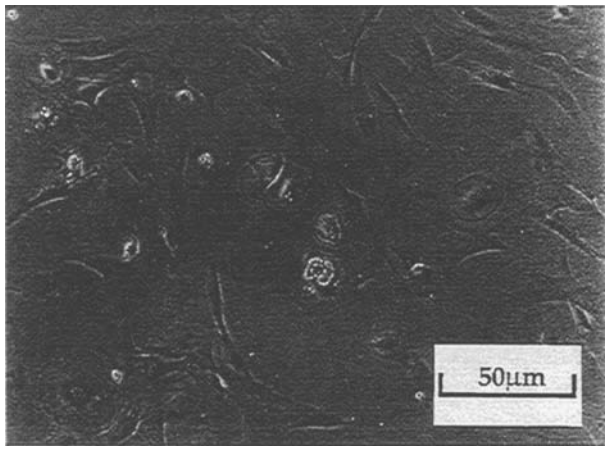

Figure 5 Phase-contrast micrograph of spindle-shaped cells, round cells and multinucleated giant cells adherent on transparent HA at 1 week after implantation into medullary cavity.

spindle-shaped cells increased on the samples and these cells formed multiple layers on the samples. These cells were positively stained for ALP (Fig. 6). ALP activity was strongly detected along the contour of these cells. Extracellular ALP activity was also demonstrated on the samples. These reaction products were observed in granules. SEM observation revealed that these cells attached to the samples and then produced fibres (Fig. 7).

In the course of time, changes in the number, morphological features, and distribution of round cells were not observed. These round cells were positively stained for NSE (Fig. 8). The activity was observed strongly over whole cells. Some round cells were also positively stained for TRAP. When cells were first stained for TRAP and followed by NSE, round cells were distinguished into two types: the NSE positive and TRAP negative cells, and both NSE and TRAP positive cells (Fig. 9).

MNGCs, nearly circular in outline, were often over 200 μm in length, and contained from three to more than ten nuclei. MNGCs were positively stained for both ACP and TRAP and negative for NSE (Fig. 8). ACP and TRAP activities were located in small granules throughout the cytoplasm, compatible with a lysosomal localization. SEM observation revealed that MNGCs were domed cells, with branching microprojections and were well adhered to the samples (Fig. 7). SEM observation of the samples after the removal of adherent cells revealed resorption lacunae similar to the outline of TRAP positive MNGC (Fig. 10). In the resorption lacunae, the average grain size was 0.62 ± 0.12 μm.

4. Discussion

HA is well known to be a biocompatible and bioactive material. When HA is implanted into osteogenic tissue, such as bone defects or medullary cavities, bone

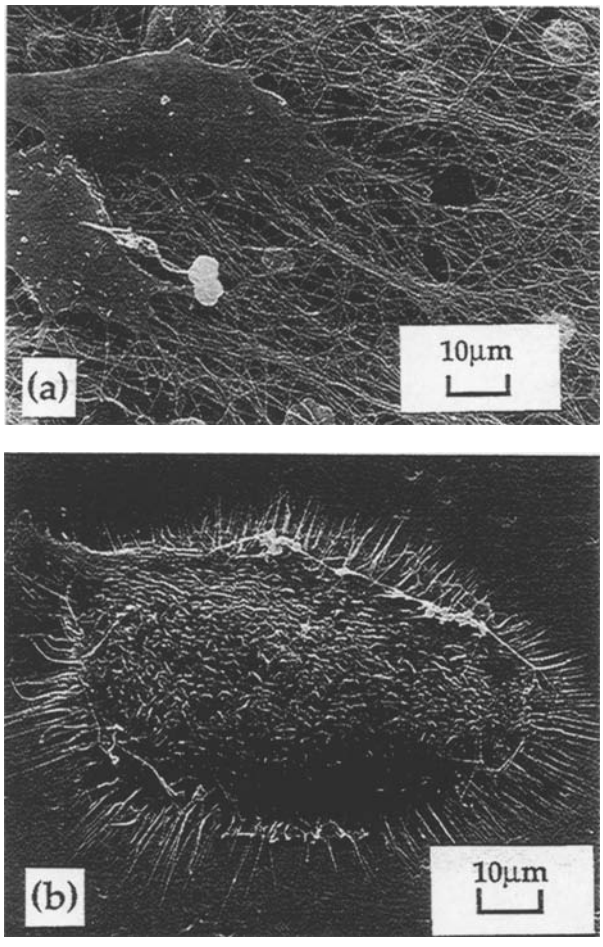

Figure 7 SEM micrographs of transparent HA surfaces at 1 week after implantation into medullary cavity: (a) production of bone matrix fibres by osteoblasts were observed; (b) osteoclast-like cell branching microprojections and well-adherent to material was observed.

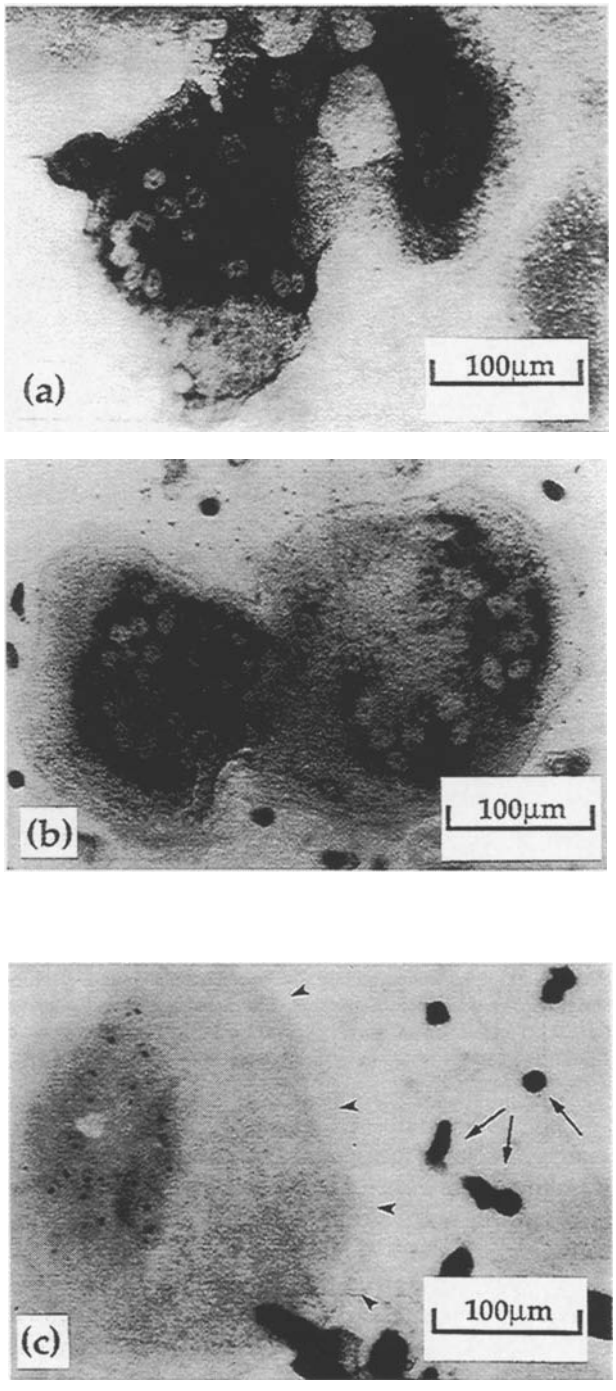

Figure 8 Acid phosphatase (ACP) (a) tartrate-resistant acid phosphatase (TRAP) (b) and nonspecific esterase (NSE) (c) staining at 1 week. (a), (b) Multinucleated giant cells (MNGCs) positive for ACP and TRAP were observed; (c) round cells (arrow) were positively stained for NSE over whole cells. Note that MNGCs (arrow head) were negative for NSE.

formation can occur on its surface and then the HA becomes directly and strongly bonded to the bone [9]. Previous reports also revealed that macrophages and MNGCs in addition to osteoblasts appear on the HA surface after implantation into osteogenic tissue. Recent reports [10, 11] on MNGCs and HA have indicated that MNGCs have morphologically and histochemically osteoclastic features. In the present study, HA/cellular interactions after implantation into medullary cavities were observed simply and dynamically by light microscopy utilizing the transparency of the HIP'ed HA, thus avoiding the necessity of histological thin sections. By utilizing enzyme reactions in the observation, histochemical identification of bone marrow derived cells responding to the implanted HA and localization of enzyme activities were revealed.

Phase-contrast microscopy revealed spindle-shaped cells, round cells, and MNGCs on the samples both at 1 week and 2 weeks after implantation. The spindle shaped cells were positively stained for ALP as a marker for osteoblasts [12] and round cells for NSE as a marker for macrophages [13]. MNGCs were positively stained for ACP and TRAP as a marker for osteoblasts [14, 15] and negatively for NSE.

Robison [16] reported that osteoblasts display the ALP activity. Since then, ALP has been implicated in bone formation and mineralization [16, 17]. Between adjacent osteoblasts, and osteoblasts and osteocytes in bone tissue, cell membrane specializations described as gap junctions occur at contact sites [18]. This junction plays a role in intercellular communication or transport for ions and small proteins. Therefore, ALP activity and the formation of a cellular network on the HA by osteoblasts suggest the active production of bone matrix such as collagen and

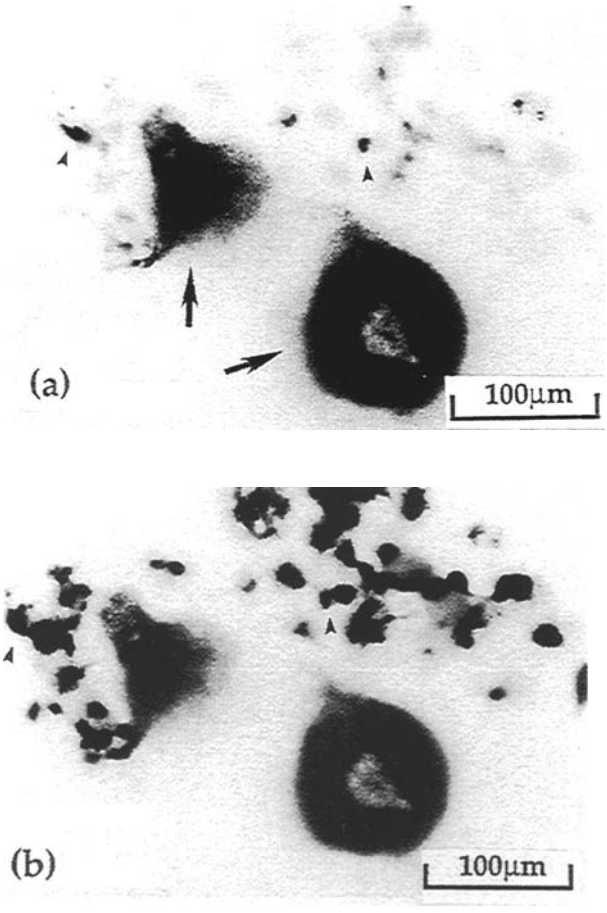

Figure 9 Double staining for tartrate-resistant acid phosphatase (TRAP) and nonspecific esterase (NSE) at 2 weeks. With a double-staining procedure, multinucleated gaint (arrow) cells were positive for TRAP and round cells were positive for NSE; a small number of round cells (arrow head) were positive for both NSE and TRAP.

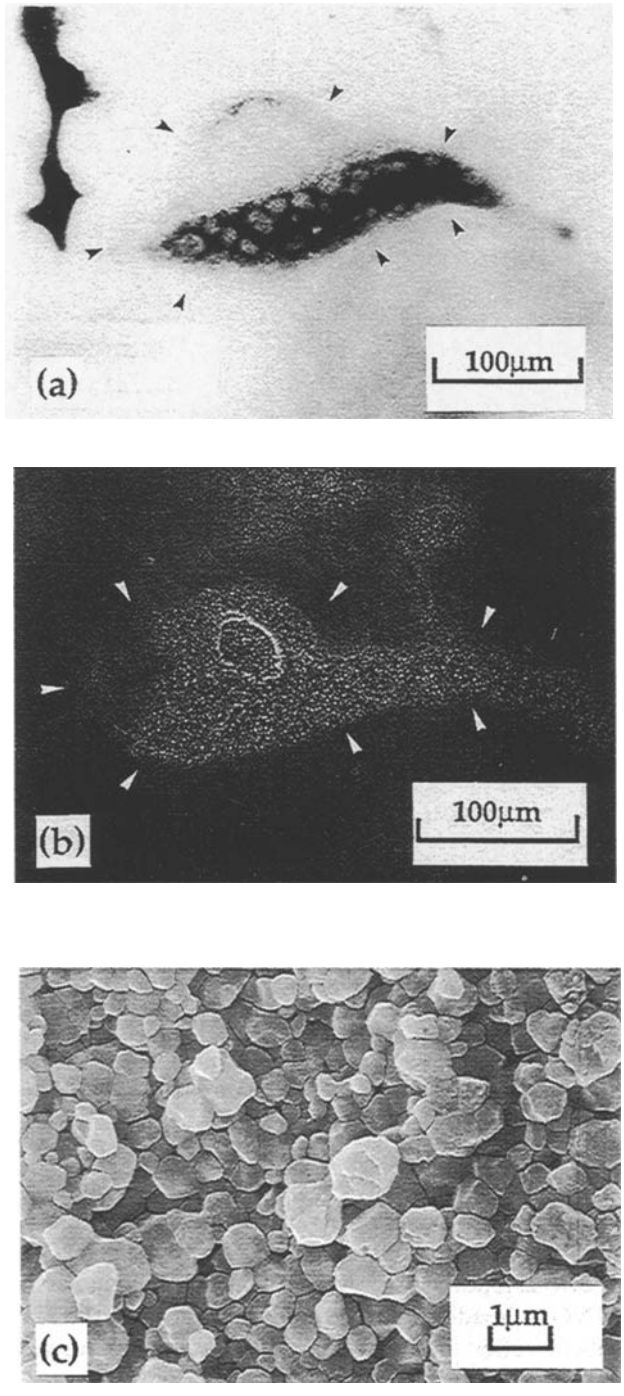

Figure 10 Positive identification of osteoclast: (a) light micrograph of multinucleated gaint cell (MNGC) positive for tartrate-resistant acid phosphatase (TRAP) at 2 weeks; (b) scanning electron micrograph revealed resorption lacunae similar to outline TRAP positive MNGC; (c) high power view of a portion of lacunae shown in (b). Average grain size was 0.62 ± 0.12 μm.

matrix vesicles. Transparent HA gave a better understanding of the adherence of osteoblasts to the dense HA surface, both morphologically and histochemically.

It is generally agreed that osteoclasts display ACP activity in bone. Hammarström [14] demonstrated that osteoclasts can be distinguished from other cells in bone by the presence of ACP which is resistant to inhibition by sodium tartrate. Minkin [15] proposed the use of TRAP as a histochemical marker for osteoclasts. Kawaguchi *et al.* [10] studied the cytochemical properties of MNGCs appearing after HA implantation into experimental osseous defects produced in rat periodontal tissues by a electron microscopy. They reported that the MNGCs demonstrated TRAP activity. Akagi *et al.* [11] demonstrated TRAP activity of MNGCs responding to HA implanted in rat mandible by a light microscopy with decalcified thin sections. By utilizing the transparency of the HIP'ed HA, the localization of TRAP activity over the whole length of the MNGCs was observed.

The present study demonstrated that the osteoclasts resorbed dense HA. SEM observation of the samples after the removal of adherent cells showed resorption lacunae similar to the outline of osteoclasts. In the resorption lacunae the average grain size was 0.62 ± 0.12 μm. The grain size of the etched surface was 0.42 ± 0.17 μm, which indicates active resorption of the smaller surface grains of HA by osteoclasts.

A number of studies have suggested that osteoclasts are formed by fusion of mononuclear precursors derived from hematopoietic progenitor cells [19]. Baron *et al.* [20] demonstrated that mononuclear cells stained for both NSE and TRAP appear *in vivo* during osteoclast formation. They suggested that decreases in the monocytic characteristics, such as NSE activity, and increases in osteoclastic nature, such as TRAP activity, occur in the progenitor cells during their

differentiation. The present study also demonstrated mononuclear cells stained for both NSE and TRAP on the HA. The existence of osteoclast precursor cells at 2 weeks after implantation suggests the continuing formation of the osteoclasts on the HA.

In vivo bone formation and resorption occur simultaneously. This remodelling phenomenon is mainly controlled by osteoblasts and osteoclasts. The appearance of osteoblasts and the resorption of the HA by osteoclasts on the HA after implantation into medullary cavity seems to be a similar phenomenon to the remodelling system in bone. It is considered that these findings suggest the biocompatibility of HA after implantation into the osteogenic tissue. Transparent HA may be a useful material for studying the coupled phenomenon of osteoblasts and osteoclasts in a bone remodelling system.

Acknowledgements

The present study was carried out under the guidance of Professor Hideki Aoki in the authors' department. The authors are grateful to Professor Hideki Aoki for his advice in making this study possible and to Professor Masahiro Yoshimura at the Tokyo Institute of Technology for use of HIP apparatus. The authors thank Dr Shizuko Ichinose, Dr Atsuo Ito, Dr Masataka Ohgaki, Dr Satosi Nakamura and Mr Kazutake Yoshizawa for their technical advice.

References

1. H. AOKI, in "Science and medical application of hydroxyapatite", edited by H. Aoki (Japanese Association of Apatite Science, Tokyo, 1991) p. 101.
2. S. FUJIWARA, M. YOSIMURA, T. HATTORI, H. AOKI, M. UCHIDA and S. SOMIYA, *Yogyo-Kyokai-Shi* **95** (1987) 753.
3. K. IOKU, S. SOMIYA and M. YOSIMURA, *J. Ceram. Soc. Jpn.* **96** (1988) 109.
4. H. AOKI, M. KIKUCHI, S. OKAYAMA, M. OHGAKI, M. AKAO, R. OTSUKA, M. KAKIHANA, M. YOSHIMURA and M. HIGASHIKATA, *Reports Inst. Med. Dent. Eng.* **26** (1992) 23.
5. C. M. MÜLLER-MAI, C. VOIGT and U. GROSS, *Scanning Microscopy* **4** (1990) 613.
6. M. S. BURSTONE, in "Enzyme histochemistry" (Academic Press, New York, 1962) pp. 88–113.
7. M. AKAO, H. AOKI and K. KATO, *J. Mater. Sci.* **16** (1981) 809.
8. M. AKAO, N. MIURA and H. AOKI, *Yogyo-Kyokai-Shi* **92** (1984) 78.
9. K. KATO, H. AOKI, T. TABATA and H. AOKI, *Biomater. Med. Dev. Artif. Org.* **7** (1979) 291.
10. H. KAWAGUCHI, T. OGAWA, M. SHIRAKAWA, H. OKAMOTO and T. AKISAKA, *J. Periodontal Res.* **27** (1992) 48.
11. T. AKAGI, N. TAKESHITA, T. NOJIMA, T. OZEKI, O. FUJII, Y. IWAMA and S. NARUGAMI, *Jpn. J. Oral Biol.* **33** (1991) 275.
12. S. YOSHIKI, T. UMEDA and Y. KURAHASHI, *Histochemie* **29** (1972) 296.
13. C. Y. LI, K. W. LAM and L. T. YAM, *J. Histochem. Cytochem.* **21** (1973) 1.
14. L. E. HAMMARSTRÖM, J. S. HANKER and S. U. TOVERUD, *Clin. Orthop. Relat. Res.* **78** (1971) 151.
15. C. MINKIN, *Calcif. Tissue Int.* **34** (1982) 285.
16. R. ROBISON, *Biochem. J.* **17** (1923) 286.
17. H. FLEISCH and W. F. NEUMAN, *Amer. J. Physiol.* **200** (1961) 1296.
18. S. B. DOTY, *Calcif. Tissue Int.* **33** (1981) 509.
19. P. J. NIJWEIDE, E. H. BURGER and J. H. M. FEYEN, *Physiol. Rev.* **66** (1986) 855.
20. R. BARON, L. NEFF, P. TRAN VAN, J. R. NEFUSSI and A. VIGNERY, *Amer. J. Pathol.* **122** (1986) 363.

Received 15 August
and accepted 7 September 1995